Available online at www.sciencedirect.com
ScienceDirect
Materials Research Bulletin 43 (2008) 2544–2553
Materials Research Bulletin
www.elsevier.com/locate/matresbu

Influence of cobalt phase on thermal shock resistance of Al_2O_3–TiC composites evaluated by indentation technique☆

Shi Rui-Xia[a,b,*], Yin Yan-Sheng[b], Li Jia[a], Wang Dong-Zhi[a]

[a] School of Materials Science and Engineering of University of Jinan, Jinan, Shandong 250022, China
[b] School of Materials Science and Engineering of Ocean University of China, Qingdao, Shandong 266100, China

Received 20 June 2006; received in revised form 31 October 2007; accepted 6 November 2007
Available online 13 November 2007

Abstract

Cobalt-coated Al_2O_3 and TiC powders were prepared using an electroless method to improve resistance to thermal shock. The mixture of cobalt-coated Al_2O_3 and TiC powders (about 70 wt.% Al_2O_3–Co + 30 wt.% TiC–Co) was hot-pressed into an Al_2O_3–TiC–Co composite. The thermal shock properties of the composite were evaluated by indentation technique and compared with the traditional Al_2O_3–TiC composite. The composites containing 3.96 vol.% cobalt exhibited better resistance to crack propagation, cyclic thermal shock and higher critical temperature difference (ΔT_c). The calculation of thermal shock resistance parameters (R parameters) shows that the incorporation of cobalt improves the resistance to thermal shock fracture and thermal shock damage. The thermal physic parameters are changed very little but the flexure strength and fracture toughness of the composites are improved greatly by introducing cobalt into Al_2O_3–TiC (AT) composites. The better thermal shock resistance of the composites should be attributed to the higher flexure strength and fracture toughness.

Keywords: A. Composites; B. Ceramics; C. Mechanical properties; D. Microstructure

1. Introduction

Ceramic materials possess excellent high temperature resistance. However, the brittleness, higher elastic modules, bad plastic deformation ability and lower thermal conductivity of ceramic materials lead them to be sensitive to environments in which the temperature fluctuates rapidly. Therefore, the full exertion of high temperature resistance of ceramic materials depends on the resistance to thermal shock. Al_2O_3–TiC (AT) composites are a kind of important engineering ceramics and have been widely used in various engineering fields [1–3]. In many applications the Al_2O_3–TiC composites are often exposed to rapid temperature changes, which might cause severe thermal stress and thermal shock damage due to their lower strength and bad thermal properties. Consequently, how to improve the thermal shock resistance of AT composites has been an important issue in their structural applications.

It has been known that the incorporation of metal phase into alumina matrix can bring about improvement on mechanical properties, including thermal shock performance [4–7]. Yet, in order to guarantee the higher hardness the

☆ Sponsored by the Doctoral Fund of Shandong Province (Grant No. 2006BS04037), National Nature Science Fund of China (Grant No. 50572034), and the Primary Program of University of Jinan (Y0602).
* Corresponding author at: School of Materials Science and Engineering of University of Jinan, Jinan, Shandong 250022, China. Tel.: +86 531 82765983; fax: +86 531 87974453.
E-mail address: mse_shirx@ujn.edu.cn (R.-X. Shi).

0025-5408/$ – see front matter © 2007 Elsevier Ltd. All rights reserved.
doi:10.1016/j.materresbull.2007.11.001

Table 1
Thermal physic parameters of Al_2O_3, TiC and cobalt

Materials	α ($\times 10^{-6}$ K^{-1})	k (W/m K)	E (GPa)	ν
Cobalt	12.5	100	210	0.31
TiC	7.4	22	462	0.19
Al_2O_3	8.8	26	380	0.26

content of metal phase is very low. The few metal phases cannot be homogeneously dispersed in matrix by using traditional technology, which results in serious metal particles agglomeration. The powder coating technique has been proved to be an effective method in processing ceramic–ceramic composites [8,9]. It was found to greatly improve the homogeneity and sinterability of composites, and consequently their mechanical properties and thermal shock resistance.

Comparing with Al_2O_3 and TiC, cobalt possesses a unique set of thermal physical properties (see Table 1), e.g. higher thermal conductivity and lower Young's modulus, which contributes to the improvement of thermal shock resistance of Al_2O_3–TiC–Co composites (ATC). In the research, the ATC composites were prepared from the cobalt coating powders that were obtained by a newly developed coating technique, which was expected to improve the mechanical and thermal shock resistance.

The thermal shock resistance of ATC composite was evaluated by indentation-quench technique and parallel reference experiments were conducted with AT composites. In order to assess specially the effects of cobalt phase on thermal shock behavior, four thermal shock parameters (R parameters) were introduced for the two composites in terms of their mechanical and physical properties.

2. Experimental procedures

2.1. Material preparation and mechanical properties

The Al_2O_3 (average particle size ~40 nm) and TiC (average particle size ~130 nm) powders were coated with cobalt film (about 3.96 vol.%) by using electroless method, respectively. In the chemical deposition method, $CoSO_4{\cdot}7H_2O$ is reduced by NaH_2PO_2 to form a thin film of cobalt on the surface of Al_2O_3 and TiC, respectively. The two kinds of ceramic powder were mixed at a ratio of 70 wt.% Al_2O_3–Co to 30 wt.% TiC–Co and homogenized by ultrasonic dispersion as the starting powders (provided by copartners of Ningbo Lingri Surface Engineering Co. Ltd., Zhejiang, China). Then the starting powders were hot-pressed in vacuum at 1650 °C for 30 min under a pressure of 30 MPa (Model HIGH MULTI 5000, FUJI DENPA, Japan). As a comparison study, Al_2O_3–TiC composites (about 70 wt.% Al_2O_3 + 30 wt.% TiC) were prepared in the same sintering process. The hot-pressed bodies were cut into bars, ground and polished to 1 μm finish before flexure strength and fracture toughness testing. Five samples were tested for either flexure strength or fracture toughness. The flexure strengths were measured in three-point test (3 mm × 4 mm × 36 mm in size); fracture toughness tests were performed by the single edge notched beam (SENB) method (2 mm × 4 mm × 36 mm in size) at a loading rate of 0.5 mm/min with a notch (2 mm in depth and 0.25 mm in width) and a span of 20 mm; and HD-187.5 Brinell tester was used to test hardness. Relative density was measured by Archimedes method. The phase composition of the polished samples was identified using X-ray diffractometry (XRD; Model D/max-rA, Rigaku Co., Japan) using Cu Kα radiation.

2.2. Indentation thermal shock

The indentation thermal shock technique developed by Andersson and Rowcliffe [10] was used to study the thermal shock and thermal fatigue behavior of the materials. In this technique, the thermal shock resistance is measured by studying the propagation of median/radial cracks around a Vickers indentation after single or repeated quenching. The specimens for thermal shock were disk shaped, with a diameter of ~30 mm and a thickness of 3 mm (Fig. 1a), with parallel 1 μm polished surfaces. Three specimens were tested for each composite. The four indentations were made uniformly, using a load of 294 N, on polished surfaces of each specimen. The holding time of each indentation was 5 s, and the interval between successive indentations was 60 s. Each indentation comes into being four cracks (Fig. 1b).

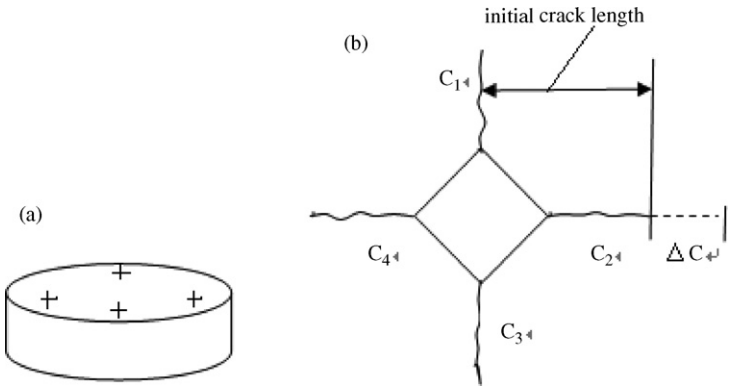

Fig. 1. (a) The sample for indentation-quench technique. (b) Schematic of Vickers indentation crack.

The quenching experiments were performed in a vertical tube furnace in air. The specimens were inserted into a preheated furnace at the testing temperatures and then were held there for 30 min before they were quenched into a bath of water (~25 °C). The test was conducted at temperature differences, ΔT, of 100–200 °C. The radial crack lengths of each indentation were measured using optical microscopy before and after quenching. To study the thermal fatigue behavior of two composites, repeated thermal shocks (up to 15 cycles) were performed for selected ΔT value of 100 °C. The fracture surfaces and indentation cracks propagation were investigated using a scanning electron microscope (SEM; Model S-2500, Hitachi).

3. Results and discussion

3.1. Mechanical properties and microstructure

Fig. 2 shows the XRD analysis of ATC composite. The final phases are Al_2O_3, TiC and cobalt, in which Al_2O_3 and TiC are major phases. The basic properties of the composites produced are summarized in Table 2. The two composites made in this study are almost fully dense. A linear intercept method has been used to evaluate the grain size of AT and ATC composites [11]. The grain sizes are also shown in Table 2. ATC composites have a smaller mean grain size than AT composites. This suggests that the grain growth in ATC is suppressed by cobalt particles that pin grain boundaries.

Hardness, flexure strength and fracture toughness of the two composites are also presented in Table 2. Hardness of ATC composites decreases slightly with addition of the cobalt phase. However, there is significant improvement in either flexure strength or fracture toughness of the ATC composites over that of AT composites.

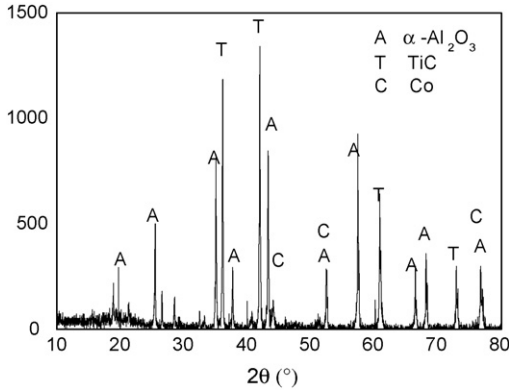

Fig. 2. XRD pattern of sintered ATC.

Table 2
Composites date and properties

Composites	Al_2O_3 (vol.%)	TiC (vol.%)	Cobalt (vol.%)	Relative density (g cm^{-3})	Grain size (μm)	Hardness (HRA)	Flexure strength (MPa)	Fracture toughness (MPa $m^{1/2}$)
AT	74.2	25.8	/	98.7	2.9	92.8	412 ± 65	4.10 ± 0.60
ATC	71.28	24.76	3.96	99.5	2.4	92.7	782 ± 60	7.81 ± 0.80

It is well known that the thermal expansion mismatch led to residual comprehensive stress between TiC particles and Al_2O_3 matrix, which is considered to be the primary toughening mechanism of AT composites [3]. Fig. 3 shows the typical SEM micrographs of the fracture surfaces of AT and ATC composites. The fracture surface of ATC shows a large proportion of transgranular cracks with some intergranular type (Fig. 3a), unlike the intergranular fracture mode of AT (Fig. 3b). In addition, cracks have been observed in the fracture surface of ATC composites (Fig. 3c), where TiC particles play an effective role in crack branching, bridging and deflection. It is suggested that cobalt phase improves interfacial bonding, leading to the change of fracture mode. This shows that the addition of 3.96 vol.% cobalt to AT composites can change the fracture mode of the AT from predominantly intergranular to transgranular.

3.2. Indentation thermal shock

Two parameters, namely fraction of cracks propagated, $\%P$, and crack extension, $\%E$, are defined as follows [12]:

$$\%P = \frac{\Delta N}{N} \times 100 \tag{1}$$

where N(=48) is the total number of available radial cracks around the indentation and ΔN the number of radial cracks propagating after thermal shock loading.

$$\%E = \frac{\Delta c}{c} \times 100 \tag{2}$$

where c is the average indentation crack length before thermal shock loading and Δc is the average crack length extended after thermal shock loading; only cracks which extended are considered in calculating $\%E$.

Table 3 and Fig. 4 summarize crack growth behavior in the AT and ATC composites after single quenching into a bath of water (~25 °C). The data show that $\%P$ and $\%E$ are dependent on ΔT, and the higher ΔT, the higher $\%P$ and $\%E$. From temperature difference 100 to 200 °C, the AT composites exhibit poor crack growth resistance after a single thermal shock, in that $\%P$ and $\%E$ are higher than for ATC composites. The partly cracks run through the surfaces for the two composites at temperature difference 200 °C.

Fig. 5 shows the Vickers indentation SEM micrographs of the two composites before and after thermal shock. The indentation shapes of ATC are more intact than ones of AT no matter what are before or after thermal shock.

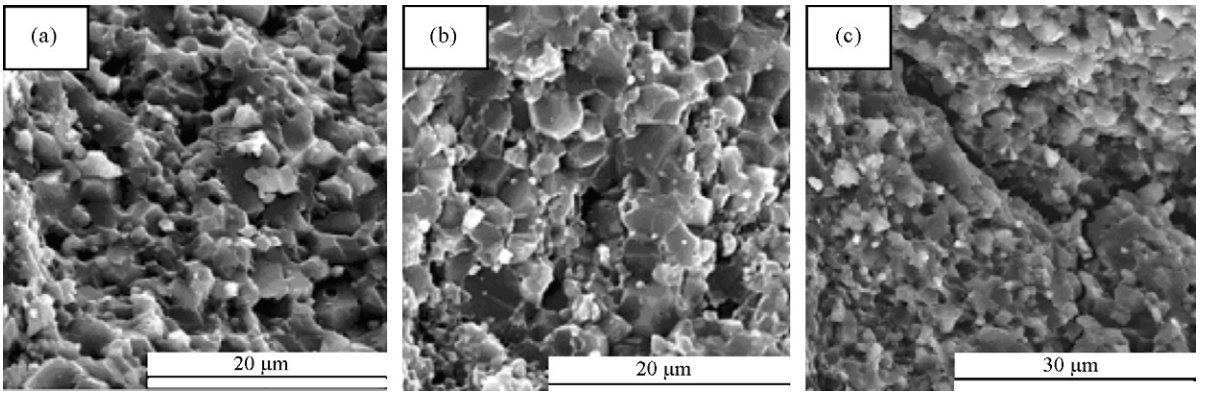

Fig. 3. SEM micrographs of the fracture surfaces: (a) AT composites (b) and (c) ATC composites.

Table 3
Crack growth data for single thermal shocks

Composites	Crack growth									
	ΔT = 100 °C		ΔT = 125 °C		ΔT = 150 °C		ΔT = 175 °C		ΔT = 200 °C	
	%P	*%E*	*%P*	*%E*	*%P*	*%E*	*%P*	*%E*	*%P*	*%E*
ATC	18.8	11.9	50	14.5	62.5	19.7	66.7	24.3	100	[a]
AT	25.0	14.5	58.3	23.7	68.8	33.3	77.1	41.4	100	[a]

[a] Denotes partly cracks run through the whole sample surface.

Fig. 6 shows the indentation crack propagation SEM micrographs of the two composites. The ATC composites show better crack propagation resistance than AT composite no matter what are before or after thermal shock. The crack propagation routes of ATC composites are more winding than those of AT composites no matter what are before or after thermal shock. There are more TiC particles that play a role in crack bridging in ATC composites than in AT composites. Moreover, there are some TiC particles that play a role in crack branching in ATC composites. As mentioned above, the presence of the cobalt phase could, to some extent, promote the crack bridging and branching of TiC particles. The ATC composites show better resistance to thermal shock than AT composites.

Table 4 and Fig. 7 show crack propagation after repeated thermal shocks, at ΔT value of 100 °C. With cycles increasing crack propagation accelerated. The all indentation cracks of the two composites propagated after 15 cycles. The AT composites are more sensitive to repeated thermal shock. The surface of AT composites was spalled (Fig. 8) under thermal stress, which is the weakness of the kind of material in utilization. The ATC shows better resistance to repeated indentation fatigue.

Thermal shock of ceramics includes the fracture initiation and cracks propagation. The theory of cracks propagation is based on Hasselman research [13]. The theory divides the relationship between flexure strength and thermal shock temperature difference into three ranges. When thermal shock temperature difference (ΔT) is lower than critical temperature difference (ΔT_c) the flexure strength keeps the original value. When ΔT is equal to ΔT_c the flexure strength degrades quickly. When ΔT is higher than ΔT_c the flexure strength keeps a constant. The thermal shock behaviors of all ceramic materials possess the characterizations above mentioned. The different ceramic material only shows different critical temperature difference (ΔT_c). *%P* and *%E* are dependent on ΔT and, the higher ΔT, the higher *%P* and *%E* [12]. The critical temperature difference ΔT_c can be quantitatively defined with reference to *%P* and *%E* as the lowest temperature difference where two criterions are simultaneously fulfilled. The one is that average extension of the crack is >10% of the original length (this criterion ensures that the crack extension is larger than any measurement errors). The other is that more than 25% of indentation cracks propagate (this criterion eliminates chance growth of single cracks and ensures statistically significant data of crack growth). According to the two criterions, ΔT_c is 100 °C for AT and 125 °C for ATC. For a thermally

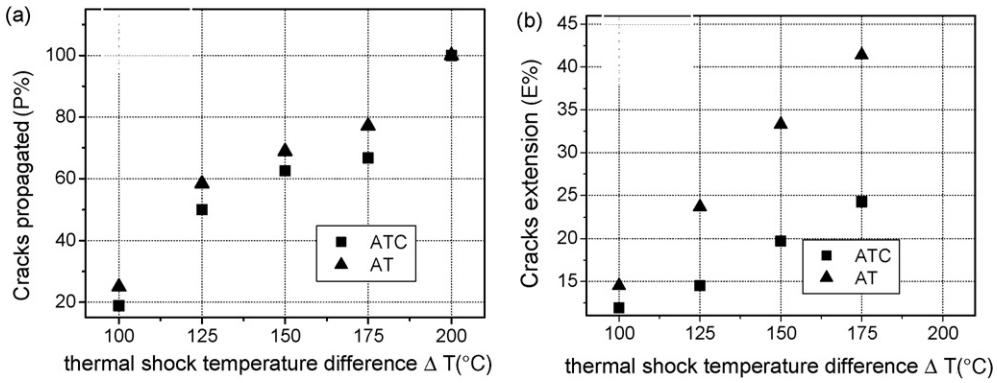

Fig. 4. Crack growth behavior in AT and ATC composites after single thermal shock: (a) fraction of cracks propagated *%P* and (b) extension in length of propagated cracks *%E*.

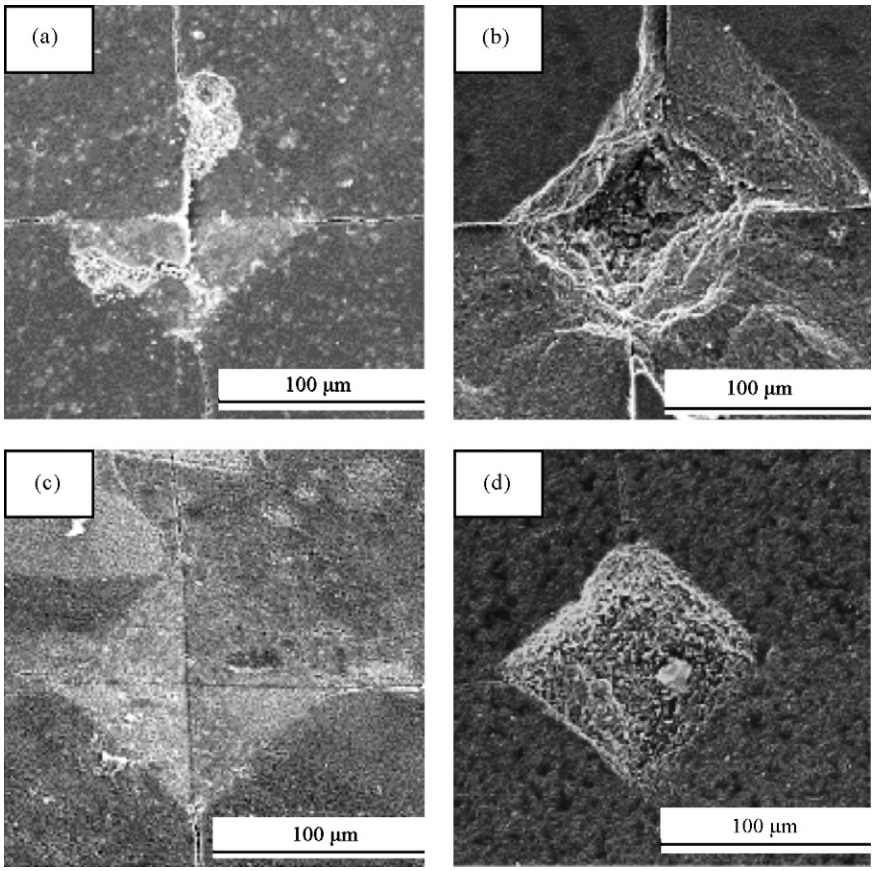

Fig. 5. SEM images of Vickers indentation crack before and after thermal shock: (a) AT before thermal shock and (b) AT after thermal shock: ($\Delta T = 200\ ^{\circ}C$). (c) ATC before thermal shock and (d) ATC after thermal shock ($\Delta T = 200\ ^{\circ}C$).

shocked ceramic material, a critical ΔT_c for a sudden temperature changes is given by the following equations [14]:

$$\Delta T_c = \frac{\sigma_f(1-\nu)}{E\alpha}\frac{1}{f(\beta)} \tag{3}$$

$$\frac{1}{f(\beta)} = \left(1.5 + \frac{B}{\beta} - 0.5\, e^{-C/\beta}\right) \tag{4}$$

$$\beta = \frac{th}{k} \tag{5}$$

where σ_f is the initial flexure strength, ν the Poisson ratio, B and C shape factors of samples depending on the specimen geometry, β the Biot modulus, E the Young modulus, α the thermal expansion coefficient, t a characteristic heat transfer length (half the thickness of the plate), k the thermal conductivity and h is the surface heat transfer coefficient acting between the plate and the cooling medium. $f(\beta)$ is the damping parameter of the thermal shock (ranging from 0 to 1) and is a function of the Biot modulus. For an infinite plate, Manson [15] has derived a semi-empirical equation relating β and $1/f(\beta)$ over the range $0 < \beta < 5$ as follows:

$$\frac{1}{f(\beta)} = 1.5 + \frac{3.25}{\beta} \tag{6}$$

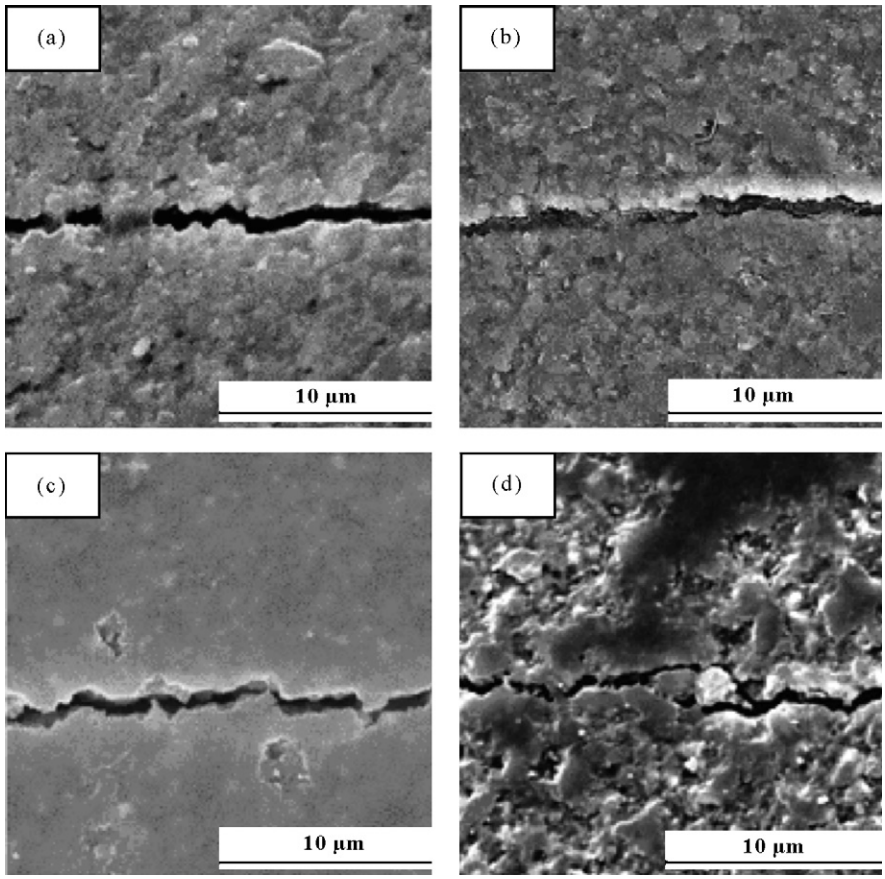

Fig. 6. SEM images of crack propagation before and after thermal shock: (a) AT before thermal shock and (b) AT after thermal shock (ΔT = 200 °C). (c) ATC before thermal shock and (d) ATC after thermal shock (ΔT = 200 °C).

Lower α and higher k result in lower thermal stress during thermal shock, consequently leading to the higher value of ΔT_c. The thermal physics parameters of AT and ATC composites (such as v, α, E and h) were assumed to be identical, and this assumption is basically reasonable for ATC composites with only 3.96 vol.% cobalt addition. And B and C the shape factors of AT and ATC composites are both identical, so the damping parameters of the thermal shock are also identical (see Eq. (4)). According to Eq. (3) the critical ΔT_c depends on flexure strength σ_f. The flexure strength σ_f can be expressed as follows [7]:

$$\sigma_f = \frac{K_{IC}}{Y\sqrt{C}} \tag{7}$$

where Y is a coefficient depending on shape and dimensions of crack and loading forms, C crack dimensions and K_{IC} is fracture toughness. Thus the critical temperature difference of ATC composites is higher than that of AT composites,

Table 4
Cyclic thermal shock crack propagation of AT and ATC composites

Material	ΔT (°C)	1 cycle		5 cycles		10 cycles		15 cycles	
		%P	%E	%P	%E	%P	%E	%P	%E
ATC	100	18.8	11.9	50.0	42.3	72.9	68.4	100	87.5[a]
AT	100	25.0	14.5	59.4	50.7	75.0	81.3	100	95.8[a]

[a] Partly cracks run through the surfaces.

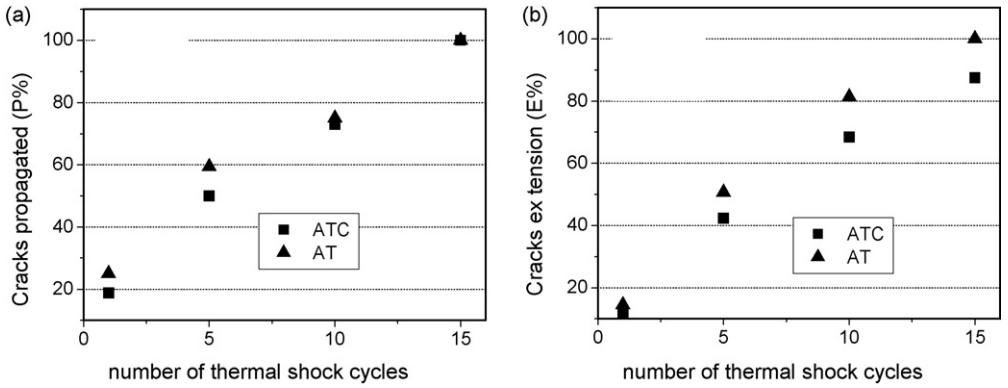

Fig. 7. Crack growth behavior in AT and ATC composites after cyclic thermal shock: (a) fraction of cracks propagated $\%P$ and (b) extension in length of propagated cracks $\%E$.

which should be mainly attributed to the higher flexure strength and fracture toughness of ATC composites (see Table 2).

The thermal shock resistance of brittle materials depends on thermal physics properties and mechanical properties. Several thermal shock parameters (R parameters) have been defined to relate these materials to their thermal resistance, considering the crack initiation and crack propagation conditions, respectively. The common used ones are defined as following [7]:

$$R = \frac{\sigma_f(1-\nu)}{\alpha E} \tag{8}$$

$$R' = kR \tag{9}$$

$$R^{IV} = \frac{E\gamma_f}{(1-\nu)\sigma_f^2} = \frac{(K_{IC}/\sigma_f)^2}{1-\nu} \tag{10}$$

$$R^{st} = \left(\frac{\gamma_f}{E\alpha^2}\right)^{1/2} \tag{11}$$

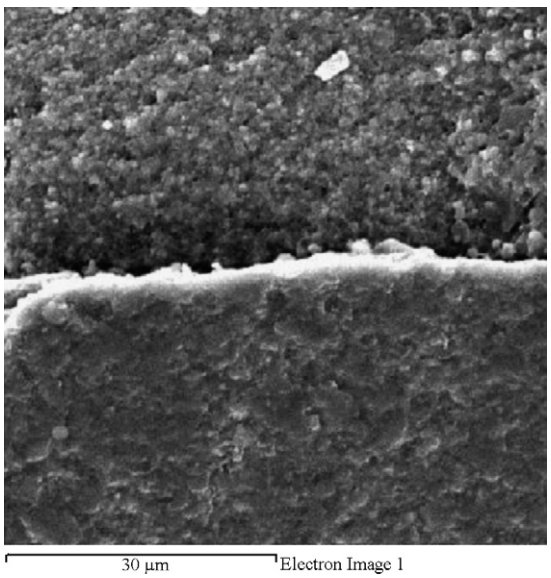

Fig. 8. Surface spalling of AT composites after cyclic thermal shock.

Table 5
Thermal physics properties and R parameters of AT and ATC composites

Materials	α ($\times 10^{-6}$ K)	k (W/m K)	E (GPa)	ν	γ_f (J/m^2	R (°C)	R' (W/m)	R^{IV} (10^{-6})	R^{st} (m$^{1/2}$ K^{-1})
AT	8.2	23.9	401	0.24	21.0	95	2271	130	0.88
ATC	8.2	23.9	401	0.24	77.4	180	4302	131	1.69

where γ_f is the surface fracture energy and other parameters were seen above. R and R' parameters predict the critical ΔT_c in a body under conditions of sharp and moderate heat or cold flow, respectively, which are expressed as the resistance to crack initiation. R^{IV} and R^{st} parameters express the ability of a material to resist crack propagation and further damage and loss of strength with increasing severity of thermal shock. Higher R^{IV} and R^{st} values indicate crack stability once the critical ΔT_c is exceeded. The calculated thermal shock parameters (R parameters) are listed in Table 5. As shown in Table 5, the calculated values of R show that the ATC composites possess a higher ΔT_c than that of AT composites, with an increase of 85 °C, which is mainly attributed to flexure strength. However, the result is higher than the experimental cure, which may be associated with the deviation of experimental data. Compared with R, there is a greater increase in R', which shows that the difference of the critical temperature difference between ATC composites and AT composites will become large when materials are under conditions of moderate heat or cold flow.

R^{IV} shows the ability of material to resist thermal shock damage. The calculated values of R^{IV} indicate that the resistance to thermal shock damage of the two composites is no distinct difference. R^{st} of ATC composites increases around 92.1% as a result of their higher surface fracture energy. According to Eq. (12) [7], material surface fracture energy is directly proportional to fracture toughness. The higher fracture toughness results in higher surface fracture energy. Therefore the higher thermal shock parameters are mainly attributed to higher fracture toughness. In addition, R^{st} is directly proportional to ΔT_c [7], which indicates critical ΔT_c of ATC composites should be higher than that of AT composites. The flexure strength and fracture toughness for ATC composites are increased by 89.8% and 90.5% in comparison to those for AT composites. The influence of 3.96 vol.% cobalt on thermal physics parameters of ATC composites are little, even it can be ignored. However, cobalt phases greatly enhance the flexure strength and fracture toughness that improves the thermal shock resistance of ATC. In a word, the better thermal shock resistance of ATC composites is mainly attributed to their higher flexure strength and fracture toughness.

$$\gamma_f = \frac{K_{IC}^2}{2E} \tag{12}$$

4. Conclusions

Indentation techniques have been successfully used to study the thermal shock behavior of AT and ATC composites. For a single thermal shock in the ΔT range 100–200 °C and repeated thermal shock in the ΔT 100 °C, an increase in thermal shock resistance over AT composites can be observed in ATC composites with an addition of 3.96 vol.% cobalt. The two composites are both sensitive to repeated thermal shock. The surface of AT composites was spalled after 15 cycles. The experimental results show that the critical temperature difference for ATC composites (~125 °C) is improved about 25 °C compared with that of AT composites (~100 °C). The calculated results of four thermal shock parameters show the ability of ATC composites to thermal shock fracture and thermal shock damage is better than that of AT composites. The thermal physics parameters of ATC composites are changed very little with adding small amounts of cobalt but the flexure strength and fracture toughness of ATC composites are greatly improved, leading them to higher thermal shock parameters. So the better thermal shock resistance of ATC composites should mainly be attributed to the enhanced strength and toughness.

References

[1] X.Q. You, T.Z. Si, N. Liu, Ceram. Int. 31 (2005) 33–38.
[2] J. Zhao, X. Ai, X.P. Huang, Mater. Process. Technol. 129 (2002) 161–166.
[3] J. Deng, T. Can, J. Sun, Ceram. Int. 31 (2005) 249–256.

[4] M.K. Aghajanian, N.H. MacMiUan, C.R. Kennedy, J. Mater. Sci. 24 (2) (1989) 658–700.
[5] S.-T. Oh, T. Sekino, K. Niihara, J. Eur. Ceram. Soc. 17 (4) (1997) 495–504.
[6] O. Sbaizero, G. Pezzotti, Acta Mater. 48 (3) (2000) 985–992.
[7] Y. Zhou, Ceramic materials, Harbin, vol. 342, Harbin Unibersity of Technology Press, China, 1995, p. 354.
[8] J. Lu, L. Gao, J. Guo, Mater. Res. Bull. 35 (2000) 2387–2396.
[9] D. Vollath, D.V. Szabo, J. Haubelt, J. Eur. Ceram. Soc. 17 (1) (1997) 1317–1324.
[10] T. Andersson, D.J. Rowcliffe, J. Eur. Ceram. Soc. 18 (14) (1998) 2065–2071.
[11] M. Li, M.J. Reece, J. Am. Ceram. Soc. 83 (4) (2000) 967–970.
[12] S. Maensiri, S.G. Roberts, J. Am. Ceram. Soc. 85 (8) (2002) 1971–1978.
[13] D.P.H. Hasselman an, J. Am. Ceram. Soc. 52 (6) (1969) 600–604.
[14] M. Collin, D. Rowcliffe, Acta Mater. 48 (2) (2000) 1655–1665.
[15] S.S. Manson, N.C.A. Technical Note 2933, Washington, D.C., 2002.